Nanoscale

Transforming Lanthanide and Actinide Chemistry with Nanoparticles

Journal:	*Nanoscale*
Manuscript ID	NR-REV-10-2019-009175.R1
Article Type:	Minireview
Date Submitted by the Author:	05-Dec-2019
Complete List of Authors:	Pallares, Roger; Lawrence Berkeley National Laboratory Abergel, Rebecca; Lawrence Berkeley National Laboratory

Minireview

Transforming Lanthanide and Actinide Chemistry with Nanoparticles

Received 00th January 20xx,
Accepted 00th January 20xx

DOI: 10.1039/x0xx00000x

Roger M. Pallares,[a] and Rebecca J. Abergel[*, a, b]

Lanthanides and actinides are used in a wide variety of applications, from energy production to life sciences. To address toxicity issues due to the chemical, and often radiological, properties of these elements, methods to quantify and recover them from industrial waste are necessary. When used in biomedicine, lanthanides and actinides are incorporated in compounds that show promising therapeutic and/or bioimaging properties, but lack robust strategies to target cancer and other pathologies. Furthermore, current decorporation protocols to respond to accidental actinide exposure rely on intravenous injections of soluble chelating agents, which are inefficient for treatment of inhaled radionuclides trapped in lungs. In recent years, nanoparticles have emerged as powerful tools in both industry and clinical settings. Because some inorganic nanoparticles are sensitive to external stimuli, such as light and magnetic fields, they can be used as building blocks for sensitive bioassays and separation techniques. In addition, nanoparticles can be functionalized with multiple ligands and act as carriers for selective delivery of therapeutic and contrast agents. This review summarizes and discusses recent progress on the use of nanoparticles in lanthanide and actinide chemistry. We examine different types of nanoparticles based on composition, functionalization, and properties, and we critically analyze their performance in a comparative mode. Our focus is two-pronged, including the nanoparticles free of lanthanides and actinides that are used for the detection, separation, or decorporation of f-block elements, as well as the nanoparticles that enhance the inherent properties of lanthanides and actinides for therapeutics, imaging and catalysis.

1. Introduction

Lanthanides and actinides are series of elements with atomic numbers from 57 to 71 and from 89 to 193, respectively. Because their f-electron shells are gradually filled as the atomic number increases (4f for lanthanides and 5f for actinides),[1] these elements are known as f-block elements (**Figure 1**). Lanthanides have large ionic radii, which decrease as the atomic number increases.[1] This ionic shrinkage is known as the "lanthanide contraction" and affects their molecular interactions and speciation. Nevertheless, their compounds show remarkable consistent properties across the series because all lanthanides preferentially adopt the +3 oxidation state.[2] Actinides are radioactive elements and most of them are human-made.[3] Only thorium and uranium are present on the Earth surface in significant quantities,[1] while actinium and protactinium do naturally occur as decay products of ^{235}U and ^{238}U but in very small amounts,[4, 5] and natural plutonium has also been reported as a result of neutron capture by uranium but in microscopic amounts.[6] Therefore, most actinides are obtained through different synthetic processes involving the bombardment of lighter elements.

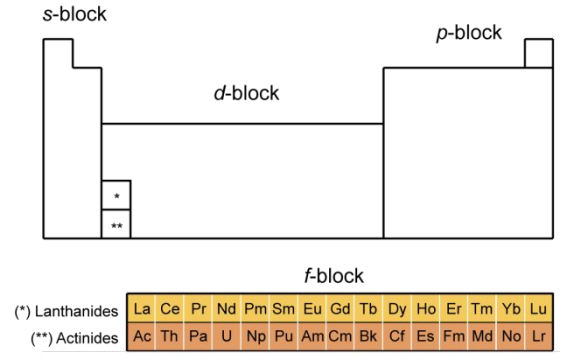

Figure 1. Location of the lanthanides and actinides in the periodic table.

[a] Chemical Sciences Division, Lawrence Berkeley National Laboratory, Berkeley, CA, 94720, USA.
[b] Department of Nuclear Engineering, University of California, Berkeley, CA, 94720, USA
*Corresponding author: abergel@berkeley.edu

Lanthanides and actinides play a major role in many human-driven activities, such as in nuclear energy,[7] clean energy technologies[8] and catalysis.[9] The processing of used nuclear fuel is particularly challenging because of the high and long-term radioactivity of minor actinides and plutonium.[10] Nuclear waste is portioned into its different components and the actinides transmuted to less hazardous isotopes. Lanthanides, however, need to be detected and removed prior to transmutation of actinides, because they quench the transmutation process through neutron-poisoning.[11] Separation of lanthanides and actinides is complicated due to their similar physical and chemical properties,[12] and significant efforts are currently being pursued to develop more efficient partitioning processes.[10, 13] Their detection in nuclear waste solutions is also challenging, since standard analytical protocols rely on instrumentation intensive in cost and time.[14] Beyond nuclear energy, the U.S. Department of Energy (DOE) has identified the lanthanides as some of the most critical materials for clean energy technologies, and new strategies involving their recovery and recycling are required to avoid future supply disruptions in the short and long terms.[15] As a result of these needs, novel approaches to detect, separate and recover f-block elements are currently being developed based on nanotechnologies. These new strategies take advantage of nanoparticles, materials with nanoscale dimensions that show high sensitivities to the presence of analytes, enhanced adsorption for separation, and responsiveness to external stimuli, such as magnetic fields.[16, 17]

In addition to energy production, lanthanides and actinides have been used in several clinical applications, including imaging and therapeutics. Imaging techniques with radionuclide-based contrast agents, such as positron-emission tomography (PET) and single-photon imaging, are regularly used to visualize pathologies that are challenging for conventional techniques like magnetic resonance imaging (MRI).[18] Because alpha radiation causes localized cell death through irreversible DNA damage, targeted alpha-particle therapy is also being developed to treat tumors.[19] In such radiotherapy modality, isotopes that undergo alpha decay are complexed with targeting molecules that deliver them to a desired treatment point. Strategies for the conjugation of these therapeutic agents with targeting molecules, however, are limited and chemically challenging. Because nanoparticles are easily biofunctionalized and enhance the delivery of the drugs inside the cells,[20, 21] the combination of f-block element complexes with nanoparticles has resulted in new opportunities for therapeutics and bioimaging. Other clinical uses of lanthanides, such as gadolinium-based contrast agents for MRI[22, 23] and probes based on lanthanide optical properties,[24] have also benefited from the latest advances in nanotechnology. Regarding optical probes, fluorescent upconverting nanoparticles doped with lanthanides should be highlighted, since they have become a rapidly growing class of nanomaterials with a wide range of biological and biomedical applications.[25]

In this review, we analyze recent progress made in the use of nanoparticles in lanthanide and actinide chemistry. We introduce different topics by summarizing the current challenges that lanthanides and actinides present, such as being the main components of some industrial wastes or when used as therapeutic and contrast agents in biomedicine. We then evaluate how different types of nanoparticles can help overcoming those issues, highlighting the most relevant properties for each application. The nanoparticles reviewed in this work are classified either as lanthanide/actinide-free nanoparticles, which are used on the sensing, separation and decorporation of f-block elements, or nanoparticles that contain these elements and enhance their native properties for biomedicine or catalysis. Finally, we comment on future opportunities nanoparticles may hold in the field of f-elements. Because this mini review is an overview of the field highlighting the recent progress, we also recommend other older reviews focused on some of the specific topics covered in this manuscript, including nanoparticles for f-element separation[26] and sensing,[27] theranostics,[24] and catalysis.[28]

2. Classes of Nanoparticles

The properties of materials change when their sizes are decreased to the nanoscale.[29] The high surface-to-volume ratio of nanoparticles can lead to several order-of-magnitude higher reactivity than what is observed in bulk materials. Furthermore, because of their unique optical, electronic, mechanical, and physico-chemical properties,[30] nanoparticles have found applications in multiple fields, from medicine to catalysis.[31-33] Among the large variety of nanoparticles developed over the last two decades, those with magnetic, plasmonic or fluorescent features are the most widely used.

Magnetic nanoparticles can be manipulated by an external magnetic field according to Coulomb's law.[31] Magnetic fields can penetrate through complex matrixes, including waste waters and biological tissues, allowing multiple applications such as magnetic separation, or magnetic tagging of biological entities.[34] Iron oxide nanoparticles, such as Fe_2O_3 and Fe_3O_4, are the most common magnetic nanoparticles because of their well-established syntheses and biocompatibility.[35]

Plasmonic nanoparticles show localized surface plasmon resonances, which result in size- and shape-dependent optical and electrical properties.[36] The intense electromagnetic near-field around the particle surface together with their strong light scattering has been used in biosensing,[37-40] imaging[41, 42] and therapeutics.[43-45] Gold nanoparticles are the most frequently used plasmonic particles because of their straightforward and scalable syntheses, as well as their biocompatibility when functionalized.[42] Furthermore, multiple morphologies (including spheres,[46] rods[47, 48] and stars[49]) with distinct properties are synthetically available.

Quantum dots are single crystal semiconductors of few nanometers in size that allow tuning of absorption and emission properties as functions of size and composition.[50] The size-dependent properties are the result of the so-called quantum confinement: when the size of the crystals is below twice the Bohr exciton radius (on the scale of a few nanometers), the

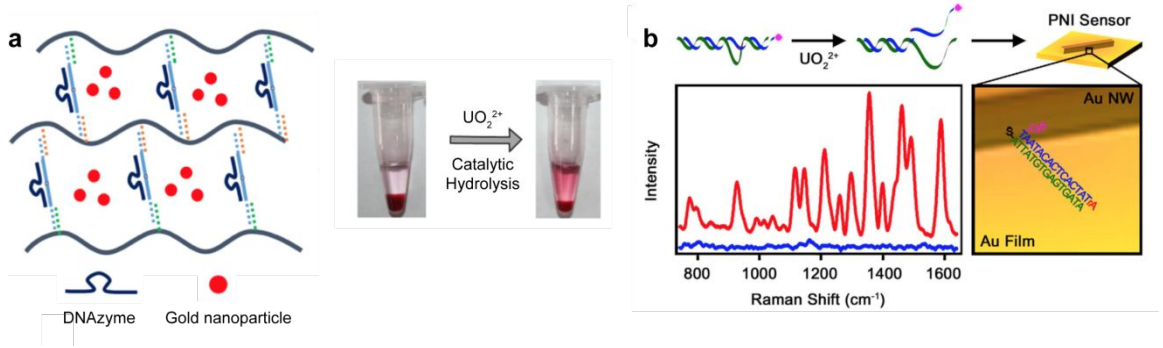

Figure 2. Sensing of UO_2^{2+} with metal nanoparticles and DNAzymes. (a) Scheme of gold nanoparticle-encapsulated hydrogel for portable detection of uranyl. Adapted with permission from ref 67. Copyright 2016 Elsevier. (b) Scheme of SERS sensor based on gold nanowires and DNAzymes. Adapted with permission from ref 70. Copyright 2016 Springer Nature.

energy levels of the quantum dots are quantified and proportional to their size. Quantum dots are advantageous over organic fluorophores because of their longer lifetimes and lack of photo-bleaching.[51] Defects within their structure, however, result in intermittent emission (blinking), which hampers some applications such as live-tracking of biological species.[52]

Upconverting nanoparticles are another class of fluorescent particles,[25] which show photon upconversion (the absorption of two or more photons is followed by the emission of a photon with higher energy). The most emission-efficient upconverting nanoparticles are those doped with rare-earth elements.[25] Thanks to their lack of blinking and bleaching, they have become the most promising alternative to organic fluorophores[53, 54] and quantum dots in bioimaging[55] and sensing[56] applications.

Finally, polymer nanoparticles are widely used as drug delivery systems because of their stability and ease to load with therapeutic agents.[57] The main synthetic protocols to prepare the nanoparticles include solvent evaporation, dialysis, salting-out, emulsions, and interfacial polymerization.[58, 59] The synthetic route chosen depends on the particle size and properties needed for the final application.[60, 61]

3. Applications of Nanoparticles

3.1. Nanoparticles for Lanthanide and Actinide Sensing

One of the few naturally-occurring actinides, uranium is among the most toxic elements present in the environment,[62] and its detection in soils and water requires sensitivities of at least parts per million[63] usually obtained through high-end, costly instrumentation, which requires intensive sample preparation procedures.[14] Multiple nanoparticle-based assays have been developed as rapid and less expensive alternatives for uranium and uranium oxide quantification. As an example, the quenching of quantum dot (CdSe/CdS core-shell) emission in the presence of uranium by electron-transfer processes was used for the development of a fluorescence assay with a limit of detection of 74.5 ppb.[64] By optimizing ligand loading on the nanoparticle, the limit of detection of the assay was further improved to 10 ppb,[65] which is lower than the limit established by the World Health Organization for uranium in drinking water (30 ppb).[66] Beyond quantum dots, the most common nanoparticle-based assays for uranium rely on noble metal nanoparticles. Huang *et al*. developed a gold nanoparticle-encapsulated hydrogel for portable detection of uranyl.[67] The hydrogel was crosslinked with DNAzyme (DNA sequences with catalytic performance that usually require metal ions as cofactors[68]), which was uranyl responsive. The presence of the dioxo cation of uranium triggered hydrogel cleavage and subsequent release of gold nanoparticles, which could then be detected by the naked eye (**Figure 2a**). A sensing chip was developed with a limit of detection of 37 nM by replacing gold nanoparticles with platinum ones.[67] This method was further expanded to detect lanthanides in solution with similar sensitivities (limit of detection of 20 nM for Ce^{3+}).[69] DNAzymes were also employed to detect uranyl ions using gold nanowires through surface-enhanced Raman spectroscopy (SERS).[70] Because SERS is a more sensitive technique than colorimetric assays, the detection limit of the sensor was improved, down to 1 pM (**Figure 2b**). Although gold is more stable, silver provides better plasmonic enhancements.[71] Hence, Jiang *et al.* developed a SERS assay for uranyl, using silver nanorods coated with alumina in order to improve the silver stability.[72] The lack of an enzymatic amplification reaction (such as that used in DNAzyme-based assays) simplified the design but resulted in higher limit of detections, in the nM range.

Aside from uranium, nanoparticle-based assays have also been used to sense other actinides and lanthanides. For instance, the high electrocatalytic activity of ruthenium nanoparticles has been used to quantify plutonium and neptunium in aqueous solutions,[73] through differential pulse voltammetry-based techniques that are rapid (minutes) but display higher limits of detection (1.5 µM for Pu and 6.5 µM for Np) than previous assays. Carbon nanoparticles, such as fluorescent graphene quantum dots, have been used for selective sensing of Ce^{3+}, which is the only lanthanide capable of quenching the fluorescence of the graphene quantum dots through a redox mechanism.[74] This assay was very selective but showed moderate limit of detection (380 nM) compared to current state of the art (pM range).

3.2. Separation of Lanthanides and Actinides with Nanoparticles

The release of hazardous radionuclides to the environment as a result of human activity, such as refinement of nuclear fuel, processing and storage of nuclear waste, or accidents in power plants, is a big threat to both public health and the environment. Several natural and synthetic sorbents have been exploited for radionuclide sequestration, including activated carbon, ion-exchange polymers, and clay minerals.[75] Many of those, however, show very limited efficiency due to low surface area, small pore size, and weak ion adsorption.[76] Hence, many designs based on nanoparticles have emerged, taking advantage of their high surface-to-volume ratios, tunable physical properties and surface chemistry, and enhanced adsorption.[77, 78] Magnetic nanoparticles have been among the most successful nanomaterials used for separation of lanthanides and actinides in water because they can be physically directed and removed from the solution with a magnet. The simplest designs rely on iron oxide nanoparticles functionalized with well-established chelators for heavy elements, such as polyaryloamidoxime or humic acid.[79, 80] Depending on the chelator used, these particles can extract uranium from environmental samples with pH ranging from 3.5 to 9.6. To take full advantage of differences in chelator selectivity and binding performance at different pH, iron oxide nanoparticles displaying two different cleavable chelating molecules were synthesized for selective La^{3+} and uranyl separation.[81] Beyond molecular chelators, carbon-based polymers are ideal nanoparticle coatings for separation applications due to their chemical and thermal stability, and the presentation of multiple functional groups for binding. Polyacrylic acid (**Figure 3a**) and tripolyphosphate-crosslinking chitosan coatings have been used to enhance the adsorption of U(VI) through carboxylic and phosphate sorption sites, respectively.[82, 83] Bio-inspired polymers, such as mussel-inspired polydopamine (**Figure 3b**), have also been used on iron oxide nanoparticles to enrich solutions with low uranium concentrations (parts per billion) with adsorption efficiencies of 99.8%.[84] The polymer coating of the magnetic nanoparticles could be replaced by carbon nanomaterials rich in nitrogen and oxygen binding sites, such as nitrogen-rich graphite (**Figure 3c**), which showed sorption capabilities between 32 and 47 mg/g for U(VI), Th(IV) and Eu(III).[85] Furthermore, these particles could be recycled, preserving sorption performance after several cycles. Composites displaying negatively-charged binding sites (hydroxyl and carboxyl groups) have also been employed, such as that formed with carboxymethyl cellulose, iron oxide nanoparticles, and carbon nanotubes.[86] The combination of the three components had a synergistic effect, showing higher adsorption performance than the individual components with q_{max} (mmol/g) of 0.34 for Eu(III), which was preserved after five adsorption cycles. In addition to modifying the nanoparticle ligand shell, doping the iron oxide core with manganese also improved the extraction of radionuclides from water solutions.[87, 88]

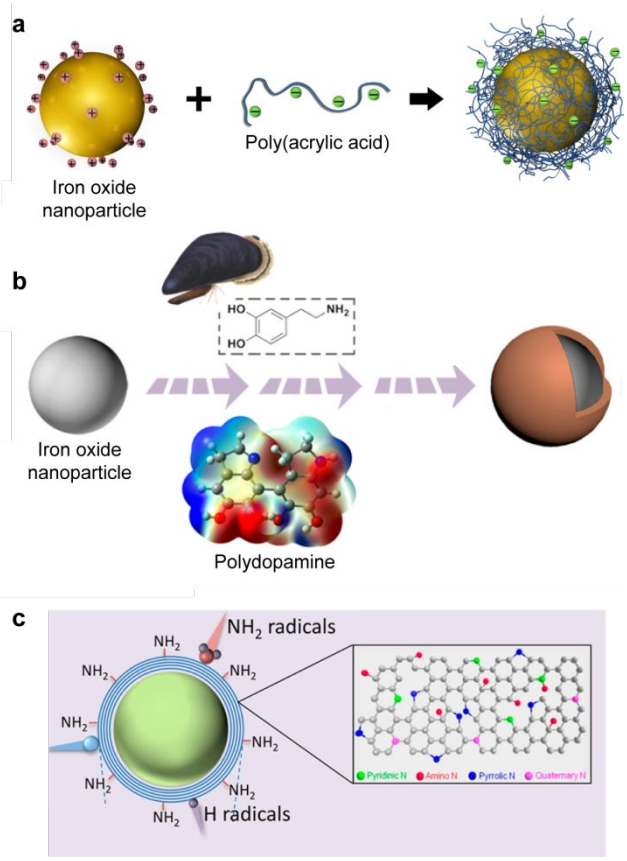

Figure 3. Magnetic nanoparticle functionalization for lanthanide and actinide separation. (a) Scheme of the coating process of positively charged iron oxide nanoparticles with negatively charged poly(acrylic acid). Adapted with permission from ref 82. Copyright 2018 Elsevier. (b) Functionalization of iron oxide nanoparticles with poly(dopamine)-inspired sorbent. Adapted with permission from ref 84. Copyright 2017 American Chemical Society. (c) Scheme of one-step arc-produced amino-functionalized graphite-encapsulated magnetic nanoparticles. Adapted with permission from ref 85. Copyright 2019 American Chemical Society.

Besides magnetic-responsive particles, non-magnetic nanoparticles made of titanium oxide or polymers have also been used for lanthanide and actinide separation.[89, 90] Upon binding, the nanoparticles formed aggregates that could be easily removed by decantation or centrifugation. By controlling the chelator displayed on the particle surface, selectivity for the heavy lanthanides was achieved (Gd/La extraction ratio of 160).[89]

3.3. Nanoparticle-based Decorporation of Actinides

Actinides, which comprise key radionuclides in the nuclear energy cycle, show both radiotoxicity and chemotoxicity.[62, 91] Once internalized, actinides are not fully excreted and accumulate preferentially in bones, liver and kidneys,[92] causing long-term irradiation hazard and ultimately chronic disease. Decorporation treatments involve intravenous injections of chelating agents, which facilitate the excretion of radionuclides through urine and feces.[93, 94] These protocols are efficient for the clearance of radionuclides in blood, but unsuccessful for the

removal of actinides trapped in the lungs after inhalation. Hence, nanoparticles made of chitosan, a water-soluble oligosaccharide that is commonly used as delivery system because of its biocompatibility and resistance to radiation and oxidation,[95] have been designed for potential use in pulmonary decorporation.[96, 97] The surface of these nanoconstructs was functionalized with chelators that showed high affinity for f-block elements. These therapeutic agents, however, are still in early stage of development and only their thermodynamics and *in vitro* performances were studied. Shi *et al.* demonstrated that in addition to chelating uranium(VI), chitosan nanoparticles containing a hydroxypyridinone-derivate ligand also scavenge uranium-induced reactive oxygen species, providing double therapeutic benefit.[98]

3.4. Nanoparticles Doped with Lanthanides and Actinides for Biomedical Applications

The photon emission of upconverting nanoparticles shows advantages over traditional fluorophores for biological applications, including enhanced tissue penetration and low photo-damage due to near-infrared excitation,[99] and absence of photo-bleaching and blinking.[99] Therefore, these nanoparticles are widely used in bio-labelling, imaging and therapeutics. Because the photoluminescence of upconverting nanoparticles is temperature sensitive, several lanthanide-doped upconverting nanoparticles have been developed as probes for nanothermometry.[100-103] In order to convert the emission intensity to temperature, a medium-specific calibration step is required. A recently developed method to predict the calibration curve based on two thermally coupled electronic level models, enables working in different media without performing multiple calibrations.[104] Although most systems show thermal quenching as the non-radiative processes are favored at higher temperatures, some nanocrystals display enhanced emission as the temperature increases. Wang *et al.* studied the thermal enhancement mechanism and identified the surface-adsorbed water molecules (and their release at higher temperatures) as the key components in the luminesce properties of the particles.[105] In addition to nanothermometry, upconverting nanoparticles have been used as labels in more conventional bioassays. For example, a bead-supported assay based on the energy transfer between upconverting nanoparticles and fluorophores was developed for miRNA quantification with limit of detection as low as fM level (**Figure 4**).[106]

Fluorescence imaging of single molecules and particles in biological media is challenging because of the high autofluorescence of tissue and body fluids. Lanthanides and lanthanide-doped nanoparticles show long luminescence lifetimes that allow time-gated imaging, reducing the autofluorescence background. For instance, poly(methyl methacrylate)-based nanoparticles encapsulating Eu^{3+} complexes were developed to image at the single particle level using illumination intensities as low as 0.24 W/cm^2 inside living cells.[107] Lanthanide-doped nanoparticles have also been

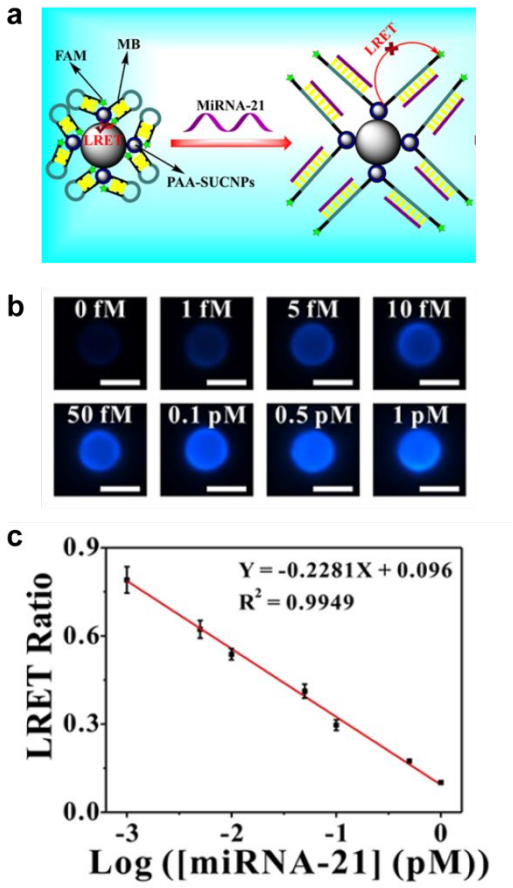

Figure 4. Sensing of miRNA with upconverting nanoparticles. (a) Scheme of the sensing principle based on luminescence resonance energy transfer (LRET) between upconverting nanoparticles and FAM dye. (b) Face-color fluorescence images and (c) response curve of the assay at different miRNA concentrations. Adapted with permission from ref 106. Copyright 2019 American Chemical Society.

engineered to display simultaneous upconverting and down-shifting emission,[108] where the particles emitted in the first and second near-infrared window, through ytterbium and thulium doping (**Figure 5**). Although both imaging modes showed comparable *in vivo* performance, down-shifting caused lower local heating because of the lower excitation power required.

Upconverting nanoparticles can also be used as delivery systems in therapeutics, such as alpha-therapy. Core-shell nanoparticles were doped with α-emitting ^{225}Ac with a shell composed by a mixture of vanadium(V) oxyanions with Eu^{3+} and Gd^{3+} that reduced the radionuclide leakage.[109] This work was in early stage, and no cell work or *in vivo* models were explored. Co-doping upconverting nanoparticles with actinides, such as ^{248}Cm, allowed to tune the light emission of the nanocrystals, as well as to obtain radioactive nanomaterials applicable to targeted radiotherapeutics.[110] Although upconversion based on actinides is not as explored as the one based on lanthanides, because of the complexity of working with radioactive materials, we expect further advances will come in the future as targeted radiotherapeutics and theranostics keep developing.

More conventional use of upconverting nanoparticles in therapeutics exploit the particle excitation by NIR light, which shows higher tissue penetration compared to visible light.[111] In

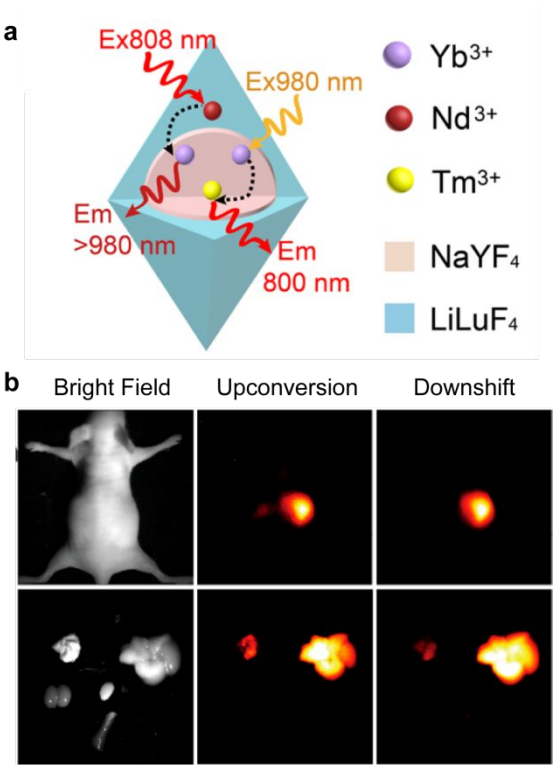

Figure 5. Upconverting nanoparticles doped with Yb and Tm show simultaneous upconversion and downshifting mechanism for NIR emission. (a) Structure of core-shell nanoparticles with dual emission. (b) *In vivo* and *ex* vivo imaging of a mouse with the upconverting nanoparticles. Adapted with permission from ref 108. Copyright 2019 American Chemical Society.

this case, nanoparticles are functionalized by photoactivatable compounds that release the therapeutic agent upon irradiation. Following this principle, nanoconstructs have been developed that release siRNA for stem cell differentiation control[112] or immunoactive DNA for immunotherapy[113]. Alternatively, the energy transfer between the upconverting nanoparticles and a photosensitizer located on the particle surface could be used to produce reactive oxygen species locally for cancer photodynamic therapy[114] and pollutant treatment of industrial waters.[115] Finally, nanoparticles for theranostics with good performance in both bioimaging and production of reactive oxygen species were obtained by engineering the crystal structure with ytterbium and thulium.[116]

Beyond upconverting nanoparticles, the combination of carbon-based nanoparticles and metals (particularly Gd) has become a subject of increasing interest in recent years.[117-120] For instance, numerous studies have explored the use of gadofullerenes as contrast agents. In these, fullerenes (*i.e.* carbon allotropes whose molecule is made of carbon atoms connected by single and double bonds forming a spheroidal mesh) are functionalized with peptides and other biomolecules for preferential accumulation in tumors.[121, 122] PET isotopes, such as ^{64}Cu or ^{89}Zr, have also been added to the gadofullerene surface through polyethylene glycol amine functionalization, resulting in simultaneous MRI contrast and PET probe capacities.[123] Because fullerenes show radical scavenger properties, gadofullerenes have been applied as theranostic nanoconstructs for imaging and therapeutic anti-inflammatory activity.[124]

3.5. Lanthanide-based Nanoparticles for Catalysis

Ceria (CeO_2) plays a major role in several industrial catalytic reactions, including carbon monoxide oxidation, diesel soot oxidation, and nitrophenol reduction.[125] The high catalytic performance of CeO_2 originates from the oxygen vacancy defects created from shifting between the oxidation states Ce(III) and Ce(IV).[126] Enhanced redox performance is obtained when the size of ceria is reduced to nanoscale,[127] and by

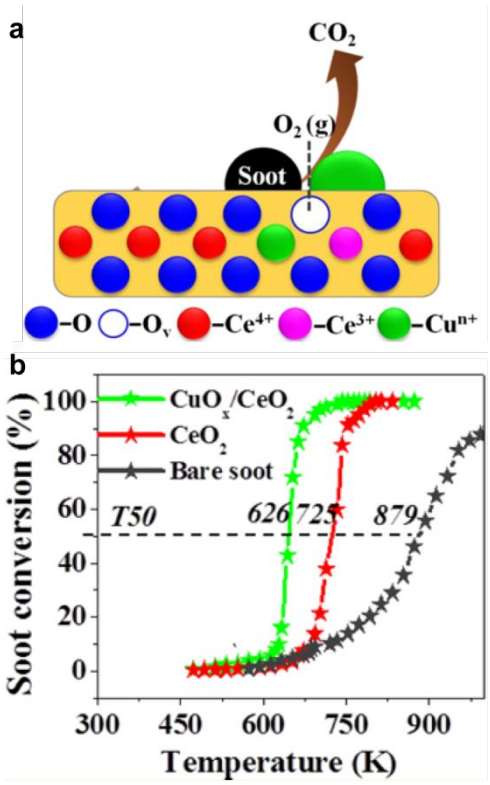

Figure 6. The oxygen vacancy defects of CeO_2 induce high catalytic performance. (a) Scheme of oxidation of diesel soot on CuO_x-decorated CeO_2 nanoparticles. (b) Comparison of soot conversion versus temperature by different substrates. Adapted with permission from ref 130. Copyright 2018 Elsevier.

combining the material with noble metals.[125] Nanoparticles made of noble metals are catalytically active and when combined with ceria, trigger a synergistic effect that occurs at the interface, with ceria acting as catalytic promoter.[126, 128, 129] For instance, CuO-decorated CeO_2 nanoparticles catalyzed diesel soot oxidation at much lower temperature than CeO_2 nanoparticles alone (**Figure 6**).[130] Because CuO-CeO_2 catalysts tend to deactivate when exposed to automotive exhaust gases at high-temperatures, the catalytic oxidation of carbon monoxide was achieved by depositing the nanoparticles on heat-resistant SiO_2 microspheres.[131] A CeO_2 shell on Ag and Pd bimetallic nanoparticles enhanced the selectivity of the catalytic reactions, such as alkyne semihydrogenation, by tuning the electronic state of the metal surface.[132]

Although not as common as cerium, other lanthanides have also been used in catalysis. Escudero-Escribano *et al.* enhanced the oxygen reduction activity of platinum electrodes through the lanthanide contraction.[133] Platinum alloys with lanthanides and alkaline earth elements were initially fabricated, and the compressive strain that resulted from leaching the lanthanides from the electrode surface resulted in 3- to 6-fold electrocatalytic enhancements. This principle was later expanded to electrodes containing platinum nanoparticles alloyed with praseodymium, achieving 3.5-fold higher activity than platinum commercial electrodes.[134]

4. Summary and Outlook

Lanthanides and actinides play a key role in many fields, including nuclear energy, catalysis and biomedicine. Because they show chemical and radiotoxicity, tools capable to quantify and extract them from industrial waste are necessary. Furthermore, conventional decorporation strategies to respond to accidental human exposure rely on intravenous treatments, which are inefficient for the clearance of lanthanides and actinides trapped in the lungs after inhalation. When applied to biomedicine, lanthanide and actinide complexes are used as probes for imaging, including MRI and PET, and therapeutics, such as targeted radionuclide-therapy. Selective strategies to target tumors and other pathologies with those therapeutic complexes, however, are still complex and uncommon.

Nanoparticles have emerged in the last couple decades as high performing building blocks for a wide variety of applications. Their high surface-to-volume ratios and interactions with external stimuli, such as magnetic fields or light, allows them to be used in sensing and separation processes. In addition, their functionalization with targeting biomolecules is exploited in the selective delivery of therapeutic agents.

In this comprehensive review, we summarize the recent progress of nanoparticles in lanthanide and actinide chemistry. The nanoparticles include those free of lanthanides that are used for the detection, separation, or decorporation of f-block elements, as well as nanoparticles that enhance the inherent properties of lanthanides for therapeutics, imaging and catalysis. In order to understand the possible impact of nanoparticles in lanthanide and actinide chemistry, we analyze current challenges of the field, and the advantages and limitations that different types of nanoparticles offer. By systematically evaluating the different applications, we believe this review will help to inform current status of the field as well as to identify future research opportunities, such as catalysis beyond ceria and upconversion of actinides, which could be exploited for theranostics.

Acknowledgments

The authors acknowledge support from the Nuclear Regulatory Commission under Faculty Development Grant NRC-HQ-84-14-G-0052 and from the U.S. Department of Energy, Office of Science, Office of Basic Energy Sciences, Chemical Sciences, Geosciences, and Biosciences Division at LBNL under Contract DE-AC02-05CH11231, during the writing of this review.

Notes and references

1. S. Cotton, *Lanthanide and Actinide Chemistry*, John Wiley & Sons, West Sussex, England, 2006.
2. D. G. Karraker, *J. Chem. Educ.*, 1970, **47**, 424.
3. L. R. Morss, N. M. Edelstein and J. Fuger, *The Chemistry of the Actinide and Transactinide Elements*, Springer, Dordrecht, The Netherlands, 2006.
4. G. J. P. Deblonde and R. J. Abergel, *Nature Chem.*, 2016, **8**, 1084.
5. Y. Asmerom, H. Cheng, R. Thomas, M. Hirschmann and R. L. Edwards, *Nature*, 2000, **406**, 293-296.
6. C. A. Levine and G. T. Seaborg, *J. Am. Chem. Soc.*, 1951, **73**, 3278-3283.
7. M. I. Ojovan and W. E. Lee, Elsevier, Oxford, Second Edition edn., 2014.
8. J. Seaman, *Rare Earths and Clean Energy: analyzing China's upper hand*, France, 2010.
9. M. S. Hill, D. J. Liptrot and C. Weetman, *Chem. Soc. Rev.*, 2016, **45**, 972-988.
10. A. Leoncini, J. Huskens and W. Verboom, *Chem. Soc. Rev.*, 2017, **46**, 7229-7273.
11. M. Salvatores and G. Palmiotti, *Progress in Particle and Nuclear Physics*, 2011, **66**, 144-166.
12. K. L. Nash, *Solvent Extr. Ion Exch.*, 1993, **11**, 729-768.
13. G. J. P. Deblonde, A. Ricano and R. J. Abergel, *Nat. Commun*, 2019, **10**, 2438.
14. T. C. Kaspar, C. A. Lavender and M. W. Dibert, *Journal*, 2017.
15. S. Chu, *Journal*, 2010.
16. S. C. N. Tang and I. M. C. Lo, *Water Res.*, 2013, **47**, 2613-2632.
17. P. K. Jain, X. Huang, I. H. El-Sayed and M. A. El-Sayed, *Acc. Chem. Res.*, 2008, **41**, 1578-1586.
18. T. I. Kostelnik and C. Orvig, *Chem. Rev. (Washington, DC, U. S.)*, 2019, **119**, 902-956.
19. Y.-S. Kim and M. W. Brechbiel, *Tumor Biology*, 2012, **33**, 573-590.
20. P. Ghosh, G. Han, M. De, C. K. Kim and V. M. Rotello, *Adv. Drug Delivery Rev.*, 2008, **60**, 1307-1315.
21. L. Dykman and N. Khlebtsov, *Chem. Soc. Rev.*, 2012, **41**, 2256-2282.
22. P. Caravan, *Chem. Soc. Rev.*, 2006, **35**, 512-523.

23. Z. Zhou and Z.-R. Lu, *Wiley Interdisciplinary Reviews: Nanomedicine and Nanobiotechnology*, 2013, **5**, 1-18.
24. H. Dong, S.-R. Du, X.-Y. Zheng, G.-M. Lyu, L.-D. Sun, L.-D. Li, P.-Z. Zhang, C. Zhang and C.-H. Yan, *Chem. Rev. (Washington, DC, U. S.)*, 2015, **115**, 10725-10815.
25. M. Haase and H. Schäfer, *Angewandte Chemie International Edition*, 2011, **50**, 5808-5829.
26. J. Veliscek-Carolan, *J. Hazard. Mater.*, 2016, **318**, 266-281.
27. M. Li, H. Gou, I. Al-Ogaidi and N. Wu, *ACS Sustainable Chemistry & Engineering*, 2013, **1**, 713-723.
28. C. Walkey, S. Das, S. Seal, J. Erlichman, K. Heckman, L. Ghibelli, E. Traversa, J. F. McGinnis and W. T. Self, *Environmental Science: Nano*, 2015, **2**, 33-53.
29. A. C. Anselmo and S. Mitragotri, *The AAPS Journal*, 2015, **17**, 1041-1054.
30. S. Mourdikoudis, R. M. Pallares and N. T. K. Thanh, *Nanoscale*, 2018, **10**, 12871-12934.
31. Q. a. Pankhurst, J. Connolly, S. K. Jones and J. Dobson, *J. Phys. D: Appl. Phys.*, 2003, **36**, R167-R181.
32. D. Bera, L. Qian, T.-K. Tseng and P. H. Holloway, *Materials*, 2010, **3**.
33. R. M. Pallares, N. T. K. Thanh and X. Su, *Nanoscale*, 2019, **11**, 22152-22171.
34. Q. A. Pankhurst, N. T. K. Thanh, S. K. Jones and J. Dobson, *J. Phys. D: Appl. Phys.*, 2009, **42**, 224001.
35. S. Laurent, D. Forge, M. Port, A. Roch, C. Robic, L. Vander Elst and R. N. Muller, *Chem. Rev. (Washington, DC, U. S.)*, 2008, **108**, 2064-2110.
36. K. L. Kelly, E. Coronado, L. L. Zhao and G. C. Schatz, *J. Phys. Chem. B*, 2003, **107**, 668-677.
37. R. M. Pallares, S. L. Kong, T. H. Ru, N. T. K. Thanh, Y. Lu and X. Su, *Chem. Commun.*, 2015, **51**, 14524-14527.
38. R. M. Pallares, M. Bosman, N. T. K. Thanh and X. Su, *Nanoscale*, 2016, **8**, 19973-19977.
39. R. M. Pallares, N. T. K. Thanh and X. Su, *Chem. Commun.*, 2018, **54**, 11260-11263.
40. R. M. Pallares, N. T. K. Thanh and X. Su, *Chem. Commun.*, 2019, DOI: 10.1039/C9CC07511A.
41. C. J. Murphy, T. K. San, a. M. Gole, C. J. Orendorff, J. X. Gao, L. Gou, S. E. Hunyadi and T. Li, *J. Phys. Chem. B*, 2005, **109**, 13857-13870.
42. S. Eustis and M. a. el-Sayed, *Chem. Soc. Rev.*, 2006, **35**, 209-217.
43. J. Yue, R. M. Pallares, L. E. Cole, E. E. Coughlin, C. A. Mirkin, A. Lee and T. W. Odom, *ACS Appl. Mater. Interfaces*, 2018, **10**, 21920-21926.
44. R. M. Pallares, P. Choo, L. E. Cole, C. A. Mirkin, A. Lee and T. W. Odom, *Bioconjugate Chem.*, 2019, **30**, 2032-2037.
45. T. B. Huff, L. Tong, Y. Zhao, M. N. Hansen, J.-X. Cheng and A. Wei, *Nanomedicine*, 2007, **2**, 125-132.
46. M. Brust, M. Walker, D. Bethell, D. J. Schiffrin and R. Whyman, *J. Chem. Soc., Chem. Commun.*, 1994, DOI: 10.1039/c39940000801, 801-801.
47. R. M. Pallares, Y. Wang, S. H. Lim, N. T. K. Thanh and X. Su, *Nanomedicine*, 2016, **11**, 2845-2860.
48. R. M. Pallares, X. Su, S. H. Lim and N. T. K. Thanh, *J. Mater. Chem. C*, 2016, **4**, 53-61.
49. R. M. Pallares, T. Stilson, P. Choo, J. Hu and T. W. Odom, *ACS Applied Nano Materials*, 2019, **2**, 5266-5271.
50. A. P. Alivisatos, *Science*, 1996, **271**, 933.
51. X. Michalet, F. F. Pinaud, L. A. Bentolila, J. M. Tsay, S. Doose, J. J. Li, G. Sundaresan, A. M. Wu, S. S. Gambhir and S. Weiss, *Science*, 2005, **307**, 538.
52. G. Yuan, D. E. Gómez, N. Kirkwood, K. Boldt and P. Mulvaney, *ACS Nano*, 2018, **12**, 3397-3405.
53. R. M. Pallares, L. Sutarlie, N. T. K. Thanh and X. Su, *Sensors and Actuators B: Chemical*, 2018, **271**, 97-103.
54. G. Hong, Y. Zou, A. L. Antaris, S. Diao, D. Wu, K. Cheng, X. Zhang, C. Chen, B. Liu, Y. He, J. Z. Wu, J. Yuan, B. Zhang, Z. Tao, C. Fukunaga and H. Dai, *Nat. Commun*, 2014, **5**, 4206.
55. Y. I. Park, K. T. Lee, Y. D. Suh and T. Hyeon, *Chem. Soc. Rev.*, 2015, **44**, 1302-1317.
56. A. Sedlmeier and H. H. Gorris, *Chem. Soc. Rev.*, 2015, **44**, 1526-1560.
57. W. B. Liechty and N. A. Peppas, *European Journal of Pharmaceutics and Biopharmaceutics*, 2012, **80**, 241-246.
58. J. P. Rao and K. E. Geckeler, *Prog. Polym. Sci.*, 2011, **36**, 887-913.
59. J. Jordan, K. I. Jacob, R. Tannenbaum, M. A. Sharaf and I. Jasiuk, *Materials Science and Engineering: A*, 2005, **393**, 1-11.
60. L. Feng, C. Zhu, H. Yuan, L. Liu, F. Lv and S. Wang, *Chem. Soc. Rev.*, 2013, **42**, 6620-6633.
61. T. Kietzke, D. Neher, K. Landfester, R. Montenegro, R. Güntner and U. Scherf, *Nat. Mater.*, 2003, **2**, 408-412.
62. A. Bleise, P. R. Danesi and W. Burkart, *J. Environ. Radioact.*, 2003, **64**, 93-112.
63. K. S. Deffeyes and I. D. MacGregor, *Scientific American*, 1980, **242**, 66-77.
64. P. Singhal, S. K. Jha, B. G. Vats and H. N. Ghosh, *Langmuir*, 2017, **33**, 8114-8122.
65. P. Singhal and V. Pulhani, *ChemistrySelect*, 2019, **4**, 4528-4537.
66. S. H. Frisbie, E. J. Mitchell and B. Sarkar, *Environmental Science: Processes & Impacts*, 2013, **15**, 1817-1823.
67. Y. Huang, L. Fang, Z. Zhu, Y. Ma, L. Zhou, X. Chen, D. Xu and C. Yang, *Biosensors and Bioelectronics*, 2016, **85**, 496-502.
68. C. E. McGhee, K. Y. Loh and Y. Lu, *Curr. Opin. Biotechnol.*, 2017, **45**, 191-201.
69. Y. Huang, X. Wu, T. Tian, Z. Zhu, H. Lin and C. Yang, *Science China Chemistry*, 2017, **60**, 293-298.
70. R. Gwak, H. Kim, S. M. Yoo, S. Y. Lee, G.-J. Lee, M.-K. Lee, C.-K. Rhee, T. Kang and B. Kim, *Scientific Reports*, 2016, **6**, 19646.
71. B. Adhikari and A. Banerjee, *Chemistry (Weinheim an der Bergstrasse, Germany)*, 2010, **16**, 13698-13705.
72. J. Jiang, L. Ma, J. Chen, P. Zhang, H. Wu, Z. Zhang, S. Wang, W. Yun, Y. Li, J. Jia and J. Liao, *Microchim. Acta*, 2017, **184**, 2775-2782.
73. R. Gupta and J. S. Gamare, *J. Electrochem. Soc.*, 2018, **165**, H277-H283.
74. F. Salehnia, F. Faridbod, A. S. Dezfuli, M. R. Ganjali and P. Norouzi, *J. Fluoresc.*, 2017, **27**, 331-338.
75. O. B. Mokhodoeva, G. V. Myasoedova and E. A. Zakharchenko, *Radiochemistry*, 2011, **53**, 35-43.
76. G. Alberti, V. Amendola, G. Bergamaschi, R. Colleoni, C. Milanese and R. Biesuz, *Dalton Trans.*, 2013, **42**, 6227-6234.
77. P. Amani, M. Amani, G. Ahmadi, O. Mahian and S. Wongwises, *Chem. Eng. Sci.*, 2018, **183**, 148-176.

78. M. Wierucka and M. Biziuk, *TrAC Trends in Analytical Chemistry*, 2014, **59**, 50-58.
79. D. Li, S. Egodawatte, D. I. Kaplan, S. C. Larsen, S. M. Serkiz and J. C. Seaman, *J. Hazard. Mater.*, 2016, **317**, 494-502.
80. P. Singhal, S. K. Jha, S. P. Pandey and S. Neogy, *J. Hazard. Mater.*, 2017, **335**, 152-161.
81. K. Wang, B. Wang, H. Li, X. Tuo, K. Xiong, M. Yan and J. Courtois, *J. Colloid Interface Sci.*, 2019, **538**, 546-558.
82. S. Zhu, Y. Leng, M. Yan, X. Tuo, J. Yang, L. Almásy, Q. Tian, G. Sun, L. Zou, Q. Li, J. Courtois and H. Zhang, *Appl. Surf. Sci.*, 2018, **447**, 381-387.
83. L. Zhou, H. Zou, Y. Wang, Z. Liu, Z. Le, G. Huang, T. Luo and A. A. Adesina, *J. Radioanal. Nucl. Chem.*, 2017, **311**, 779-787.
84. F. Wu, N. Pu, G. Ye, T. Sun, Z. Wang, Y. Song, W. Wang, X. Huo, Y. Lu and J. Chen, *Environ. Sci. Technol.*, 2017, **51**, 4606-4614.
85. J. Xiao, W. Song, R. Hu, L. Chen and X. Tian, *ACS Applied Nano Materials*, 2019, **2**, 385-394.
86. P. Zong, D. Cao, Y. Cheng, S. Wang, T. Hayat, N. S. Alharbi, Z. Guo, Y. Zhao and C. He, *Inorganic Chemistry Frontiers*, 2018, **5**, 3184-3196.
87. W. Chouyyok, C. L. Warner, K. E. Mackie, M. G. Warner, G. A. Gill and R. S. Addleman, *Ind. Eng. Chem. Res.*, 2016, **55**, 4195-4207.
88. M. J. O'Hara, J. C. Carter, C. L. Warner, M. G. Warner and R. S. Addleman, *RSC Advances*, 2016, **6**, 105239-105251.
89. R. Rahal, F. Annani, S. Pellet-Rostaing, G. Arrachart and S. Daniele, *Sep. Purif. Technol.*, 2015, **147**, 220-226.
90. V. Luca, J. J. Tejada, D. Vega, G. Arrachart and C. Rey, *Inorg. Chem.*, 2016, **55**, 7928-7943.
91. J. T. Edsall, *Bulletin of the Atomic Scientists*, 1976, **32**, 26-37.
92. B. Kullgren, E. E. Jarvis, D. D. An and R. J. Abergel, *Toxicol. Mech. Methods*, 2013, **23**, 18-26.
93. D. D. An, B. Kullgren, E. E. Jarvis and R. J. Abergel, *Chem.-Biol. Interact.*, 2017, **267**, 80-88.
94. G. N. Stradling, *J. Alloys Compd.*, 1998, **271-273**, 72-77.
95. J. J. Wang, Z. W. Zeng, R. Z. Xiao, T. Xie, G. L. Zhou, X. R. Zhan and S. L. Wang, *Int J Nanomedicine*, 2011, **6**, 765-774.
96. S. Chen, R. Ko, E. P. C. Lai, H. Wyatt, R. J. Abergel and C. Li, *Radiat. Prot. Dosim.*, 2018, **182**, 107-111.
97. L. Léost, J. Roques, A. Van Der Meeren, L. Vincent, N. Sbirrazzuoli, C. Hennig, A. Rossberg, J. Aupiais, S. Pagnotta, C. Den Auwer and C. Di Giorgio, *Dalton Trans.*, 2018, **47**, 11605-11618.
98. C. Shi, X. Wang, J. Wan, D. Zhang, X. Yi, Z. Bai, K. Yang, J. Diwu, Z. Chai and S. Wang, *Bioconjugate Chem.*, 2018, **29**, 3896-3905.
99. M. Lin, Y. Zhao, S. Wang, M. Liu, Z. Duan, Y. Chen, F. Li, F. Xu and T. Lu, *Biotechnology Advances*, 2012, **30**, 1551-1561.
100. L. Li, F. Qin, L. Li, H. Gao and Z. Zhang, *J. Mater. Chem. C*, 2019, **7**, 7378-7385.
101. O. A. Savchuk, J. J. Carvajal, C. D. S. Brites, L. D. Carlos, M. Aguilo and F. Diaz, *Nanoscale*, 2018, **10**, 6602-6610.
102. M. Back, E. Trave, J. Ueda and S. Tanabe, *Chem. Mater.*, 2016, **28**, 8347-8356.
103. P. Du, A. M. Deng, L. Luo and J. S. Yu, *New J. Chem.*, 2017, **41**, 13855-13861.
104. S. Balabhadra, M. L. Debasu, C. D. S. Brites, R. A. S. Ferreira and L. D. Carlos, *J. Phys. Chem. C*, 2017, **121**, 13962-13968.
105. Z. Wang, J. Christiansen, D. Wezendonk, X. Xie, M. A. van Huis and A. Meijerink, *Nanoscale*, 2019, **11**, 12188-12197.
106. C.-Y. Li, Y.-F. Kang, C.-B. Qi, B. Zheng, M.-Q. Zheng, C.-Y. Song, Z.-Z. Guo, Y. Lin, D.-W. Pang and H.-W. Tang, *Anal. Chem.*, 2019, **91**, 7950-7957.
107. M. Cardoso Dos Santos, A. Runser, H. Bartenlian, A. M. Nonat, L. J. Charbonnière, A. S. Klymchenko, N. Hildebrandt and A. Reisch, *Chem. Mater.*, 2019, **31**, 4034-4041.
108. C. Cao, Q. Liu, M. Shi, W. Feng and F. Li, *Inorg. Chem.*, 2019, **58**, 9351-9357.
109. M. Toro-González, R. Copping, S. Mirzadeh and J. V. Rojas, *J. Mater. Chem. B*, 2018, **6**, 7985-7997.
110. P. Agbo, A. Müller, L. Arnedo-Sanchez, P. Ercius, A. M. Minor and R. J. Abergel, *Nanoscale*, 2019, **11**, 7609-7612.
111. A. Bagheri, H. Arandiyan, C. Boyer and M. Lim, *Advanced Science*, 2016, **3**, 1500437.
112. J. Li, C. W. T. Leung, D. S. H. Wong, J. Xu, R. Li, Y. Zhao, C. Y. Y. Yung, E. Zhao, B. Z. Tang and L. Bian, *ACS Appl. Mater. Interfaces*, 2019, **11**, 22074-22084.
113. H. Chu, J. Zhao, Y. Mi, Z. Di and L. Li, *Nat. Commun*, 2019, **10**, 2839.
114. X. Song, Z. Yue, T. Hong, Z. Wang and S. Zhang, *Anal. Chem.*, 2019, **91**, 8549-8557.
115. X. Li, K. Yang, C. Yu, S. Yang, K. Zhang, W. Dai, H. Ji, L. Zhu, W. Huang and S. Ouyang, *J. Mater. Chem. C*, 2019, **7**, 8053-8062.
116. G. Ramírez-García, E. De la Rosa, T. López-Luke, S. S. Panikar and P. Salas, *Dalton Trans.*, 2019, **48**, 9962-9973.
117. Y. Wang, S. Díaz-Tendero, F. Martín and M. Alcamí, *J. Am. Chem. Soc.*, 2016, **138**, 1551-1560.
118. R. Zhao, Y. Guo, P. Zhao, M. Ehara, S. Nagase and X. Zhao, *J. Phys. Chem. C*, 2016, **120**, 1275-1283.
119. O. Semivrazhskaya, A. Romero-Rivera, S. Aroua, S. I. Troyanov, M. Garcia-Borràs, S. Stevenson, S. Osuna and Y. Yamakoshi, *J. Am. Chem. Soc.*, 2019, **141**, 10988-10993.
120. Y. Feng, J. Li, Z. Zhang, B. Wu, Y. Li, L. Jiang, C. Wang and T. Wang, *Dalton Trans.*, 2015, **44**, 7781-7784.
121. Z. Han, X. Wu, S. Roelle, C. Chen, W. P. Schiemann and Z.-R. Lu, *Nat. Commun*, 2017, **8**, 692.
122. Y. Zhou, R. Deng, M. Zhen, J. Li, M. Guan, W. Jia, X. Li, Y. Zhang, T. Yu, T. Zou, Z. Lu, J. Guo, L. Sun, C. Shu and C. Wang, *Biomaterials*, 2017, **133**, 107-118.
123. D. Chen, Y. Zhou, D. Yang, M. Guan, M. Zhen, W. Lu, M. E. Van Dort, B. D. Ross, C. Wang, C. Shu and H. Hong, *ACS Appl. Mater. Interfaces*, 2019, **11**, 21343-21352.
124. T. Li, L. Xiao, J. Yang, M. Ding, Z. Zhou, L. LaConte, L. Jin, H. C. Dorn and X. Li, *ACS Appl. Mater. Interfaces*, 2017, **9**, 17681-17687.
125. A. Trovarelli and P. Fornasiero, eds., *Catalysis by Ceria and Related Materials*, Imperial College Press, London, 2002.
126. M. Mittal, A. Gupta and O. P. Pandey, *Solar Energy*, 2018, **165**, 206-216.
127. D. Zhang, X. Du, L. Shi and R. Gao, *Dalton Trans.*, 2012, **41**, 14455-14475.
128. X. Wang, D. Liu, J. Li, J. Zhen, F. Wang and H. Zhang, *Chemical Science*, 2015, **6**, 2877-2884.
129. Y. Liu, Q. Wang, L. Wu, Y. Long, J. Li, S. Song and H. Zhang, *Nanoscale*, 2019, **11**, 12932-12937.

130. P. Sudarsanam, B. Hillary, B. Mallesham, B. G. Rao, M. H. Amin, A. Nafady, A. M. Alsalme, B. M. Reddy and S. K. Bhargava, *Langmuir*, 2016, **32**, 2208-2215.
131. Y.-Y. Song, L.-Y. Du, W.-W. Wang and C.-J. Jia, *Langmuir*, 2019, **35**, 8658-8666.
132. S. Song, K. Li, J. Pan, F. Wang, J. Li, J. Feng, S. Yao, X. Ge, X. Wang and H. Zhang, *Adv. Mater. (Weinheim, Ger.)*, 2017, **29**, 1605332.
133. M. Escudero-Escribano, P. Malacrida, M. H. Hansen, U. G. Vej-Hansen, A. Velázquez-Palenzuela, V. Tripkovic, J. Schiøtz, J. Rossmeisl, I. E. L. Stephens and I. Chorkendorff, *Science*, 2016, **352**, 73.
134. J. Fichtner, B. Garlyyev, S. Watzele, H. A. El-Sayed, J. N. Schwämmlein, W.-J. Li, F. M. Maillard, L. Dubau, J. Michalička, J. M. Macak, A. Holleitner and A. S. Bandarenka, *ACS Appl. Mater. Interfaces*, 2019, **11**, 5129-5135.

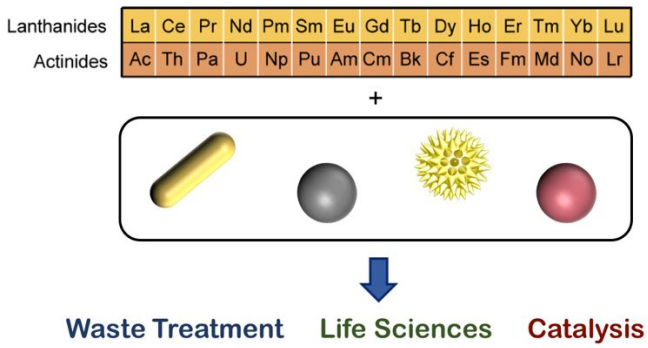
Lanthanides
La Ce Pr Nd Pm Sm Eu Gd Tb Dy Ho Er Tm Yb Lu
Actinides
Ac Th Pa U Np Pu Am Cm Bk Cf Es Fm Md No Lr
+
Waste Treatment
Life Sciences
Catalysis